

Polygonal blending splines in application to image processing

Tatiana Kravets^[0000-0002-1208-5772]

R&D group Simulations,
Department of Computer Science and Computational Engineering,
Faculty of Engineering Science and Technology,
UiT – The Arctic University of Norway, Norway

Abstract. The paper proposes a novel method of image representation. The basic idea of the method is to transform color images to continuous parametric surfaces.

The proposed technique is based on a class of special basis functions, defined on the polygon grid. Besides a flexible and symmetric construction, these basis functions are strictly local and C^d -smooth on the entire domain. Having a number of unique features, the proposed representation can be used in various image processing tasks.

The main purpose of this paper is to demonstrate the process of the image transformation and discuss possible applications of the presented technique.

Keywords: Image processing · Voronoi diagram · polygon grid · blending splines · expo-rational basis functions

1 Introduction

The proposed paper is concerned with the development of the image processing tool that expresses an image as a linear superposition of special basis functions.

The approximation technique presented in this paper is a mixture of polygon image tessellation and discrete image transformations. The processed image is decomposed into a set of pre-generated basis functions and real coefficients. The transformed image is then represented as a continuous surface, thus, a number of postprocessing techniques can be applied to that representation. For example, one can apply finite element analysis (FEA) methods to image editing [15]. In particular, B-splines were applied to image approximation [2].

Blending spline type constructions possess many possible applications, mainly in Computer Aided Geometric Design (CAGD) [14], finite element analysis (FEA) [6] and isogeometric analysis (IGA) [12], and in particular in image processing [8]. Blending splines model a freeform surface representation, where local surfaces are blended together to form global surface. There exist specialized methods for evaluating these splines over triangular grids [3, 11] and tensor-product-based grids [14]. The current paper presents a method for evaluating the general surface construction over an arbitrary polygon grid such that the

blending surface preserves C^d smoothness. One of the features of the blending spline representation is achieving an accurate approximation on relatively coarse domains keeping strict locality. This property allows us to handle abrupt color changes smoothly.

In this paper we apply blending spline techniques to image approximation. The novelty of the proposed approach is the preliminary sampling of the image (polygonalization) with the aim of further blending of local regions. Since polygonal regions are more flexible (have more degrees of freedom) than quadrilateral, the proposed approach is promising compared to the tensor product spline approximation. Polygons cover freeform regions and can potentially be adaptive to image properties: flat regions will have fewer sampling points than detailed regions.

The paper is organized as follows. Section 2 focuses on the preliminary theory which is relevant to the proposed technique. Two phases of image approximation are considered in Section 3. Section 4 presents numerical experiments and comparisons. Section 5 summarizes the proposed work and identifies research questions for future development.

2 Preliminaries

In this section we consider some of the theory regarding blending spline constructions over polygon grid which is relevant for this work.

2.1 Generalized barycentric coordinates

Let $P_n \subset \mathbb{R}^2$ be a polygon with vertices $\mathbf{v}_1, \mathbf{v}_2, \dots, \mathbf{v}_n$, $n \geq 3$. According to [9], any functions $u_i : P_n \rightarrow \mathbb{R}$, $i = 1, \dots, n$, are called generalized barycentric coordinates, if for all $\mathbf{x} \in P_n$, $u_i(\mathbf{x}) \geq 0$, $i = 1, \dots, n$, and

$$\sum_{i=1}^n u_i(\mathbf{x}) = 1, \quad \sum_{i=1}^n u_i(\mathbf{x})\mathbf{v}_i = \mathbf{x}. \quad (1)$$

One commonly used type of the generalized barycentric coordinates suitable for arbitrary polygons is called *mean value coordinates*, which are defined as

$$u_i(\mathbf{x}) = \frac{w_i(\mathbf{x})}{\sum_{j=1}^n w_j(\mathbf{x})}$$

and

$$w_i(\mathbf{x}) = \frac{\tan(\alpha_{i-1}/2) + \tan(\alpha_i/2)}{\|\mathbf{v}_i - \mathbf{x}\|}, \quad (2)$$

where the angles $\alpha_i = \alpha_i(\mathbf{x})$, $0 < \alpha_i < \pi$, are shown in Figure 1.

These coordinates are used for a mapping between local polygon coordinates and global coordinates on the parametric domain. The mapping between the

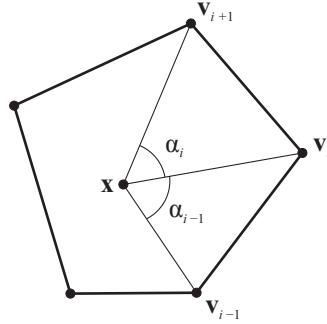


Fig. 1. Notation of the mean value coordinates.

parametric domain and the Cartesian coordinate system is achieved by a linear combination of basis functions defined in the parametric domain and control points that belong to the Euclidean space.

2.2 Combined expo-rational basis functions

A parametric function that maps the domain $\Omega \subset \mathbb{R}^2$ onto \mathbb{R}^n is constructed by the linear product of basis functions $\varphi_i : \Omega \rightarrow \mathbb{R}$ and corresponding coefficients $\zeta_i \in \mathbb{R}^n$, $i = 1, \dots, N$. In matrix form this can be written as

$$S = \zeta^T \varphi, \quad (3)$$

where S is a continuous mapping $S : \Omega \subset \mathbb{R}^2 \rightarrow \mathbb{R}^n$. Here, φ is a row vector of the basis functions, ζ is a column vector of the coefficients.

The combined expo-rational basis functions, defined in [12, 13], were developed on a foundation of the theory of the expo-rational B-splines (ERBS), firstly introduced in 2006 by L.T. Dechevsky et al. [5]. The concept of blending surfaces can be briefly described as blending of local surfaces by underlying expo-rational basis functions. Thus, the final surface possesses a hierarchical structure. However, this construction can be interpreted by formula (3), so that the functions φ_i , $i = 1, \dots, N$, are built using a combination of the underlying and local basis functions.

Let us consider the evaluation of the combined expo-rational basis functions in the one dimensional case.

Given a one dimensional domain I , which is subdivided into knot intervals with a local parameter $u \in (0, 1]$ defined on each interval. A univariate expo-rational basis function defined along the parameter u is expressed as

$$B(u) = \begin{cases} \Gamma \int_0^u \phi(s) ds, & \text{if } 0 < u \leq 1, \\ 0, & \text{otherwise,} \end{cases} \quad (4)$$

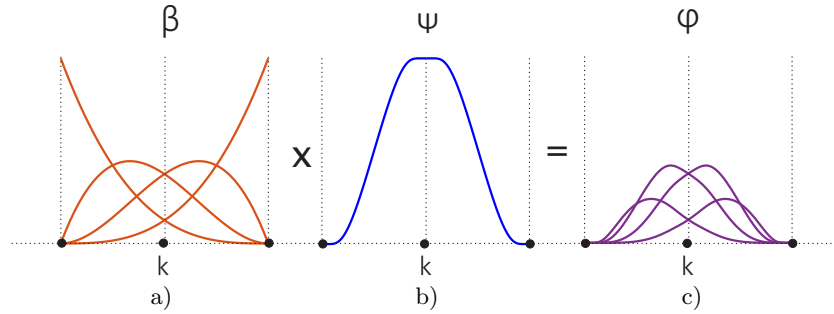


Fig. 2. Evaluation of the combined expo-rational basis functions in the one-dimensional case: β is a set of local Bézier basis functions, ψ_k is one underlying expo-rational function, φ is a product of these two sets that forms a locally defined set of the combined expo-rational basis functions.

where

$$\phi(u) = \exp\left(-\frac{(u-1/2)^2}{u(1-u)}\right),$$

and the scaling factor

$$\Gamma = \left(\int_0^1 \phi(u) du\right)^{-1}.$$

The expo-rational basis function, whose construction is based on (4), is positive, symmetric and strictly local on two neighbor knot intervals. The complete basis is evaluated as a set of these basis functions defined for each knot with local support on the neighbor knot intervals. Figure 2(b) shows one expo-rational basis function ψ_k , defined on two knot intervals having k^{th} knot as a common knot. The symmetric part of the function ψ_k is evaluated as $1 - B(u)$.

We select Bézier curves to be blended as one possible option. Bernstein polynomials form a basis for Bézier curves and surfaces. In order to blend the local Bézier curves, each curve is defined on each two neighbor knot intervals. Thus, introducing a local parameter t over two knot intervals, one can express the local Bernstein polynomials of degree d as

$$\beta_{d,\gamma} = \frac{d!}{\gamma!(d-\gamma)!} t^\gamma (1-t)^{d-\gamma}. \quad (5)$$

Figure 2(a) shows the set of Bernstein polynomials forming a basis for the local Bézier curve. In order to construct a local curve ℓ_k , where k is a knot index, we find a product of the basis functions $\beta_{d,\gamma}$ and the corresponding coefficients ζ_γ . Thus, for a complete set of local curves, we define the blending curve as a combination of the underlying basis ψ_k and the set of local curves ℓ_k . Alternatively, one can combine the underlying basis functions with the basis functions

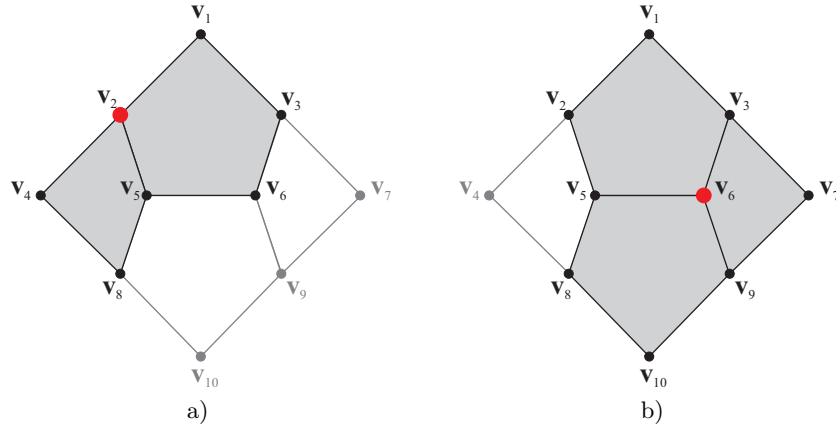


Fig. 3. An example of the polygon grid. Two groups of the polygons having one common vertex (v_2 and v_6) are shown in figures (a) and (b), respectively.

of the local curves over each two knot intervals. Then, the final basis functions with local support look like it is illustrated in Figure 2(c) and are evaluated as

$$\varphi_{(k,\gamma)} = \beta_\gamma \psi_k, \quad (6)$$

where k iterates over the knot intervals and γ iterates over the indices of the Bernstein polynomials. Let for simplicity the tuple (k, γ) be denoted as the index i . Then, a set of the combined expo-rational functions is ordered with respect to i , $i = 1, \dots, N$, where N is the total number of coefficients ζ taken from the local curves.

2.3 Polygonal blending spline construction

Now, we can directly expand the one-dimensional representation of the combined expo-rational basis functions to a multivariate form. Let β be a set of the polygonal Bézier basis functions, ψ_k be one underlying expo-rational basis function defined on a set of polygons having one common vertex with an index k . Let also \mathbf{x} be a point that belongs to a polygon $P_n \subset \mathbb{R}^2$ with n vertices.

By analogy with the one dimensional case, two knot intervals, expanded to a polygon grid, are represented as a set of polygons having one common vertex. Figure 3 demonstrates an example of the polygon grid. Two groups of polygons having one common vertex are highlighted, which correspond to the supports of the underlying expo-rational basis functions ψ_2 and ψ_6 , respectively.

A set of Bézier basis functions of degree d , defined on a polygon P_n with $n \geq 3$ sides, is given as

$$\beta_\gamma = \beta_{d,\mathbf{a}}(\mathbf{x}) = \frac{d!}{a_1! a_2! \dots a_n!} u_1^{a_1}(\mathbf{x}) u_2^{a_2}(\mathbf{x}) \dots u_n^{a_n}(\mathbf{x}), \quad \mathbf{x} \in P_n, \quad (7)$$

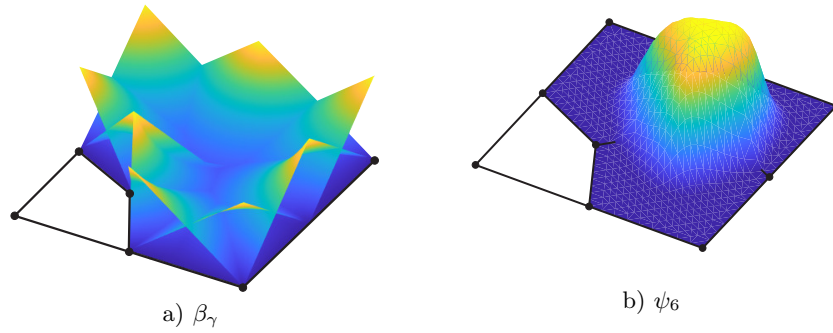


Fig. 4. Illustration of the basis functions defined on the grid shown in Figure 3. (a) A set of the Bézier basis functions of degree one defined on the set of polygons with a common vertex v_6 . (b) One underlying expo-rational function ψ_6 on its polygonal support.

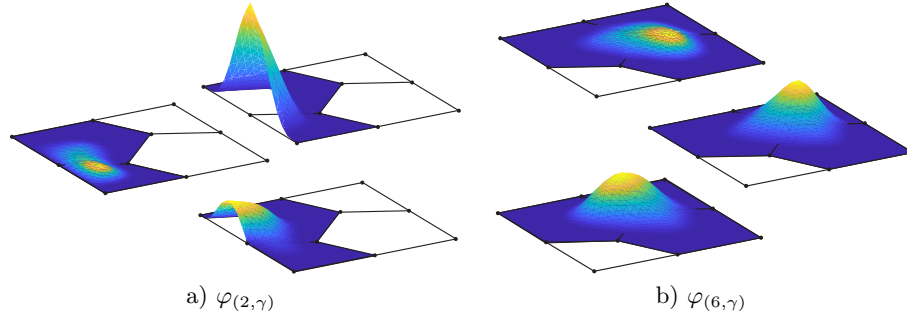


Fig. 5. Some examples of the combined expo-rational basis functions of degree one defined on the polygon grid shown in Figure 3.

where u_1, u_2, \dots, u_n is a set of generalized barycentric coordinates for the given polygon, $\mathbf{a} = (a_1, a_2, \dots, a_n)$, $a_1 + a_2 + \dots + a_n = d$, is a multi-index. The functions (7) form a basis of the Bézier polygon [10]. Note that in order to blend the local Bézier polygonal surfaces, we define them on each set of the grid polygons having one common vertex, as shown, for example, in Figure 4(a).

The underlying expo-rational basis function in generalized barycentric coordinates is defined on one polygon P_n for any $\mathbf{x} \in P_n$ as

$$\mathcal{B}(u_i(\mathbf{x})) = \frac{B(u_i)}{B(u_1) + B(u_2) + \dots + B(u_n)} \quad \text{for } i = 1, 2, \dots, n, \quad (8)$$

where $B(u_i)$ is evaluated by formula (4). Thus, each $\mathcal{B}(u_i)$ is defined for each vertex of the polygonal element such that $\mathcal{B}(u_i(\mathbf{x})) = 1$ if $\mathbf{x} = \mathbf{v}_i$ and $\mathcal{B}(u_i(\mathbf{x})) = 0$ along edges that do not contain \mathbf{v}_i . One expo-rational basis function ψ_k , which is formed as a “bell” shape, has its support on the neighbor polygons having a common vertex, and it is formed as the functions $\mathcal{B}(u_i(\mathbf{x}))$ such that they are equal to 1 at the vertex \mathbf{v}_k , and equal to zero along all edges of its support

(except the domain boundary). This property of the underlying expo-rational basis functions provides strict locality of the basis, which is especially promising for the polygonal grids in comparison with other smooth spline representations. Figure 4(b) shows the underlying basis function ψ_6 on its support.

On the polygonal grid the expo-rational basis functions are C^0 -smooth, in contrast with tensor product representation of the same basis, where the basis functions are C^∞ -smooth [7, 6, 13]. Thus, by blending using local Bernstein polynomials of degree d we obtain C^d -smoothness of the combined basis on the polygon grid inside the domain Ω .

Multiplying the underlying expo-rational basis functions ψ_k and the corresponding local Bézier basis functions β_γ over each set of the polygons having a common vertex \mathbf{v}_k , we obtain the combined expo-rational basis φ by analogy with the one-dimensional case (6). Figure 5 illustrates some examples of these basis functions, defined on the polygonal grid shown in Figure 3.

A set of the combined expo-rational basis functions forms the basis for constructing a polygonal blending surface. It is linearly independent and sums up to one at any point of the domain.

3 Image approximation

3.1 Partitioning

A natural choice of partitioning of the two dimensional domain into a set of polygons is the utilization of the Voronoi diagram. In terms of the image representation, one can select sampling points randomly, or adaptively to image properties [16]. The goal of this representation is to approximate the image colors such that one can reconstruct the original image by increasing the number of samples. In contrast, the purpose of the blending spline approximation is to achieve a better approximation on the blending phase while keeping the initial sampling as coarse as possible.

Thus, we propose a sampling technique that is based on the center of masses of the specific color regions. Let the original image be transformed to a few evenly spaced gray shades. Then we find a center of mass for each color, and a longest distance between two points in the current color region. If the farthest distance is larger than the given parameter, then we subdivide the current region to two parts by the line which is perpendicular to the line having two farthest points and goes through the center of mass. This sampling process repeats until the distance between two farthest points is less than the given parameter. Several steps of this process are shown in Figure 6(a)-(e). A set of distributed points is shown on the grayscale image in Figure 6(f).

Once the sampling points are selected we start generating Voronoi cells. An algorithm that provides clipping of the Voronoi diagram to the domain boundary and collapses the short edges to obtain more uniform partitioning is based on the `PolyMesher` generator [17]. The result of the partitioning process is shown in Figure 7.

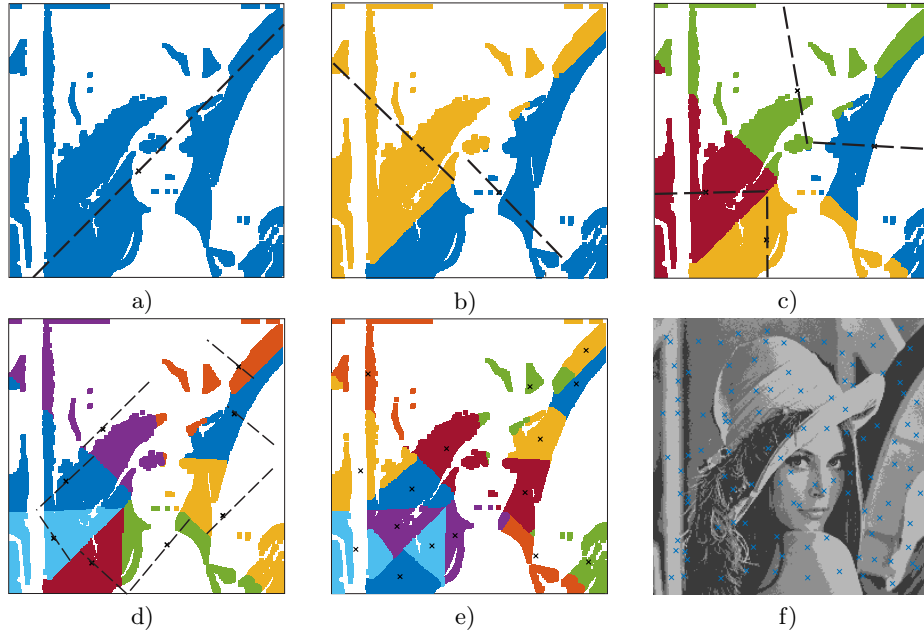


Fig. 6. (a)-(e) Sampling process. (f) Distribution of sampling points.

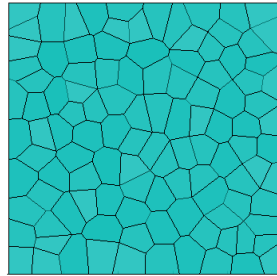


Fig. 7. Generated grid after removing short edges.

The generated cells are grouped by neighbor polygons having one common vertex. The local set of the combined expo-rational basis functions is defined on each of these groups.

3.2 L^2 -projection

We seek for the one-to-one correspondence between blending surfaces and two dimensional color images. In order to obtain this correspondence we need to project an image in the color space onto the space of the combined expo-rational basis functions.

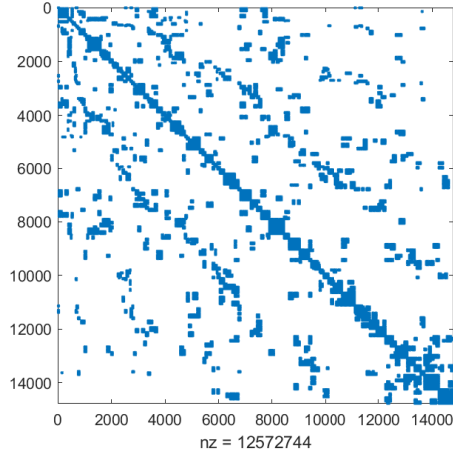


Fig. 8. Sparsity pattern of the matrix M .

Let \mathcal{V} be the space of all continuous functions spanned by the combined expo-rational basis φ_i , $i = 1, 2, \dots, N$.

An L^2 -projection $S \in \mathcal{V}$ of a function $f \in L^2(\Omega)$ is defined as

$$\int_{\Omega} (f - S)\varphi_i d\Omega = 0, \quad i = 1, 2, \dots, N. \quad (9)$$

Since S belongs to \mathcal{V} it can be written in matrix form as (3). Inserting (3) to the definition (9) we obtain

$$\int_{\Omega} (f\varphi)^T d\Omega = \zeta \int_{\Omega} \varphi^T \varphi d\Omega.$$

Introducing the notation $M = \int_{\Omega} \varphi^T \varphi d\Omega$, $b = \int_{\Omega} (f\varphi)^T d\Omega$, we get the following linear system for the unknown vector of coefficients ζ

$$M\zeta = b. \quad (10)$$

Thus, the coefficients ζ in the expression (3) that satisfy the linear system (10) give the orthogonal projection of the function f defined on the domain Ω onto the space of the combined expo-rational basis functions, in our particular case.

Figure 8 illustrates the sparsity pattern of the matrix M on the example of a grid having 128 polygons and second degree local surfaces.

4 Numerical experiments

The numerical experiments are performed on the following standard images used in digital image processing: “Lena”, “baboon” and “peppers”, shown in Figure 9.

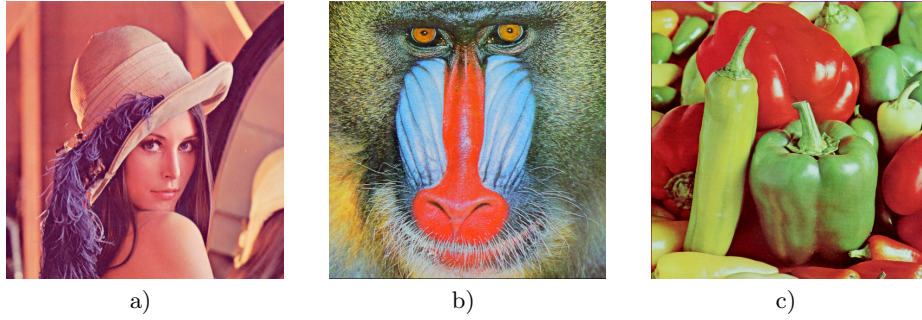


Fig. 9. (a) “Lena”. (b) “baboon”. (c) “peppers”.



Fig. 10. “Lena”, second degree local surfaces, (a) 24 elements, (b) 32 elements, (c) 128 elements.

The images have size 256×256 pixels. These images were selected in order to exploit the proposed algorithm on a variety of detail, flat and noise regions, and distribution of colors.

The peak signal to noise ratio (PSNR) is used to measure the approximated image quality and it is calculated by formula $\text{PSNR} = 10 \log \left(\frac{M_X^2}{\|f - S\|_X^2} \right)$, where M_X is the maximum possible pixel value of the image in the color representation and $\|f - S\|_X^2$ is the mean squared error of the original image f compared to its approximation S over the pixels X .

Figures 10-12 show several iterations of the presented method of image approximation. The chart in Figure 13 demonstrates the method performance. Although the algorithm does not provide a beneficial PSNR between 30-50 dB after the first few iterations, it shows a steady trend towards improving image quality as the number of elements increases. However, we suppose that alternative methods can be used to improve the image quality. For example, the blending splines preserve the derivatives at the interpolation points [7], thus, one can approximate the image gradient. In the current paper we only introduce the method based on polygonal blending splines, so its variations require additional development.



Fig. 11. “peppers”, second degree local surfaces, (a) 32 elements, (b) 128 elements.

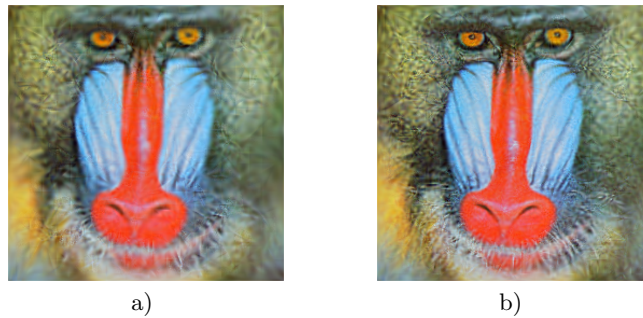


Fig. 12. “baboon”, second degree local surfaces, (a) 64 elements, (b) 128 elements.

5 Concluding remarks

This paper introduces a method for image representation by using the blending type spline construction evaluated on a polygon grid. We have shown two phases of image approximation: (i) polygon grid generation with a purpose for further blending, (ii) orthogonal projection of a colored image onto the space of the combined expo-rational basis functions. Image processing is a particular application of the proposed method. This approach is originally intended to be utilized in isogeometric analysis as an extension of the work shown in [12]. However, IGA methods can also be applied to image approximation and enhancement. If, for example, we assume that the image is a solution to some partial differential equation, then the continuous representation of the solution allows us to adjust inner parameterization such that it improves approximation.

There are several unique properties of the proposed surface construction. The most promising feature is the evaluation of a C^d -smooth surface on a polygon grid. Combined with local support of basis functions, this provides an extensive framework that can be applied to approximation of a wide range of functions defined on arbitrary polygrid topology.

Several possible applications result directly from the continuous representation of the image and the features described above. First of all, image approx-

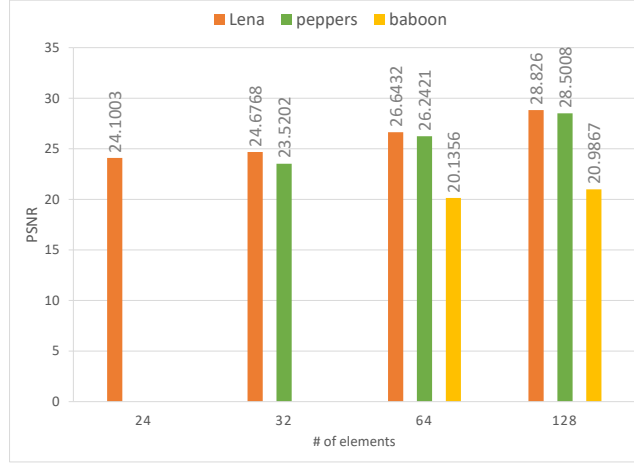


Fig. 13. Performance chart for the test images in Figures 10-12.

imation is by itself a form of image compression. For a predetermined set of basis functions, the image can be encoded as a set of approximation coefficients. An approach that shows the decomposition of an image into a set of logistic expo-rational basis functions and corresponding coefficients as applied to image compression is presented in [4]. Next, the continuous representation of an image allows us to increase its resolutions at the expense of finer discretization. Another possible application of the blending spline approximation of images is inpainting. One can fill in damaged or missing regions with approximate colors while preserving derivatives.

The main weakness of the proposed method is its computational cost. However, the issue is not in the algorithm efficiency itself, but in its optimization. The construction of the basis functions can potentially be parallelized, but it requires additional study and development.

Some possible algorithm improvements can be implemented. The first idea is to change the color space of the image from RGB to, for example, YCbCr or XYB, which is used in JPEG XL format [1]. The appropriate color space may depend on the color distribution in the image. Second, the sampling algorithm can be improved in several ways. For example, one can change the metric from Euclidean to another one, or develop a non-uniform distribution of sampling points by using an adaptive maximum distance between the farthest points in one polygon.

References

1. Alakuijala, J., Ruud van Asseldonk, Boukourt, S., Bruse, M., Comşa, I.-M., Firsching, M., Fischbacher, T., Kliuchnikov, E., Gomez, S., Obryk, R., Potempa, K., Rhatushnyak, A., Sneyers, J., Szabadka, Z., Vandevenne, L., Versari, L., Wassenberg, J.: JPEG XL next-generation image compression architecture and coding tools. Proc. SPIE 11137, Applications of Digital Image Processing XLII, 111370K, (2019)
2. Briand, T., Monasse, P.: Theory and practice of image B-Spline interpolation. IPOL - Image Processing on Line, **8**, 99–141, (2018)
3. Dalmo, R., Bratlie, J., Bang, B., Lakså, A.: Smooth spline blending surface approximation over a triangulated irregular network. International Journal of Applied Mathematics, **27**(1), 109–119, (2014)
4. Dalmo, R., Bratlie, J., Zanaty, P.: Image compression using an adjustable basis function. Mathematics in Engineering, Science and Aerospace, **6**(1), 25–34, (2015)
5. Dechevsky, L.T., Lakså, A., Bang, B.: Expo-Rational B-Splines. International Journal of Pure and Applied Mathematics, **27**(3), 319–367, (2006)
6. Dechevsky, L.T., Zanaty, P.: First instances of univariate and tensor-product multivariate generalized expo-rational finite elements. In: Applications of Mathematics in Engineering and Economics 2011, **1410**, 128–138, American Institute of Physics, (2011)
7. Dechevsky, L.T., Zanaty, P.: Smooth GERBS, orthogonal systems and energy minimization. In: Applications of Mathematics in Engineering and Economics 2013, **1570**, 135–162, (2013)
8. Dechevsky, L.T., Zanaty, P., Bang, B., Lakså, A.: Smooth partition of unity with Hermite interpolation: applications to image processing. In: Image processing: Algorithms and Systems X; and Parallel Processing for Imaging Applications II, volume **8295** of Proceedings of SPIE, page 82950C, (2012)
9. Floater, M.S.: Generalized barycentric coordinates and applications. Acta Numerica, **24**, 161–214, (2015)
10. Floater, M.S., Lai, M.-J.: Polygonal Spline Spaces and the Numerical Solution of the Poisson Equation. SIAM Journal on Numerical Analysis, **54**(2), 797–824, (2016)
11. Kravets, T.: Finite element method application of ERBS triangles. NIK2019: Norwegian Informatics Conference, (2019)
12. Kravets, T.: Representation and application of spline-based finite elements. Universitetet i Tromsø – Norges arktiske universitet, ISBN 978-82-7823-214-9, (2020)
13. Kravets, T., Dalmo, R.: Finite element application of ERBS extraction. Journal of Computational and Applied Mathematics. **379**, 112947, (2020)
14. Lakså, A.: Basic properties of Expo-Rational B-splines and practical use in Computer Aided Design. University of Oslo, PhD thesis, (2007)
15. Matias Di Martino, J., Facciolo, G., Meinhardt-Llopis, E.: Poisson image editing. IPOL - Image Processing On Line, **6** 300–325, (2016)
16. Rom, H., Peleg, S.: Image representation using Voronoi tessellation: adaptive and secure. In: Proceedings / CVPR, IEEE Computer Society Conference on Computer Vision and Pattern Recognition, 282 – 285, (1988)
17. Talischi, C., Paulino, G.H., Pereira, A., Menezes, I.F.M.: **PolyMesher**: a general-purpose mesh generator for polygonal elements written in Matlab. In: Structural and Multidisciplinary Optimization, **45**, 309–328, (2012)